SCIENTIFIC REP♦RTS

OPEN

Manipulating Steady Heat Conduction by *Sensu*-shaped Thermal Metamaterials

Tiancheng Han[1], Xue Bai[2,3,4], Dan Liu[2,3,4], Dongliang Gao[2], Baowen Li[3,4,5], John T. L. Thong[2,4] & Cheng-Wei Qiu[2,4]

The ability to design the control of heat flow has innumerable benefits in the design of electronic systems such as thermoelectric energy harvesters, solid-state lighting, and thermal imagers, where the thermal design plays a key role in performance and device reliability. In this work, we employ one identical sensu-unit with facile natural composition to experimentally realize a new class of thermal metamaterials for controlling thermal conduction (e.g., thermal concentrator, focusing/resolving, uniform heating), only resorting to positioning and locating the same unit element of sensu-shape structure. The thermal metamaterial unit and the proper arrangement of multiple identical units are capable of transferring, redistributing and managing thermal energy in a versatile fashion. It is also shown that our sensu-shape unit elements can be used in manipulating dc currents without any change in the layout for the thermal counterpart. These could markedly enhance the capabilities in thermal sensing, thermal imaging, thermal-energy storage, thermal packaging, thermal therapy, and more domains beyond.

Researchers have been pursuing effective methodologies to control thermal flux for multifarious applications[1–13]. The manipulation of heat flow is essential in technology development in many areas such as thermoelectricty[1], fuel cells[2], thermal barrier coatings[3], solar cells[4], electronics and optoelectronics[5], and low thermal conductivity materials[6]. In addition, the ability to precisely control heat flow can potentially lead to the development of thermal analogues of electrical circuit components[7], such as thermal diodes[8–10], thermal transistors[11], and thermal memory[12]. More recently, thermo-crystals were theoretically proposed for thermal management, guiding thermal wave just as photonic crystals guide light[13].

While the conduction of heat has been known for a long time, the advance in the control of heat flow has been very slow[7–16]. Most recently, by using a multilayered composite approach, cloaking, concentration, and reversal of heat flux were experimentally demonstrated in thick composites[17] and planar structures[18]. Considering that the heat conduction equation is form invariant under coordinate transformations, thermal cloaks were realized with inhomogeneous anisotropic thermal conductivities[19–21]. On the basis of exact methodology (directly solving heat conduction equation), bilayer thermal cloaks made of bulk isotropic materials have been reported[22,23]. Though significant progress has been made toward the manipulation of heat flow, different functionalities have to rely on different structures[14–24]. This motivates us to explore a general class of thermal metamaterial units, with which a set of interesting functionalities

[1]School of Physical Science and Technology, Southwest University, Chongqing 400715, China. [2]Department of Electrical and Computer Engineering, National University of Singapore, 4 Engineering Drive 3, Republic of Singapore. [3]Department of Physics and Centre for Computational Science and Engineering, National University of Singapore, Singapore 117546, Republic of Singapore. [4]NUS Graduate School for Integrative Sciences and Engineering, National University of Singapore, Kent Ridge 119620, Republic of Singapore. [5]Center for Phononics and Thermal Energy Science, School of Physics Science and Engineering, Tongji University, 200092, Shanghai, China. Correspondence and requests for materials should be addressed to T.H. (email: tchan123@swu.edu.cn) or C-W.Q. (email: eleqc@nus.edu.sg)
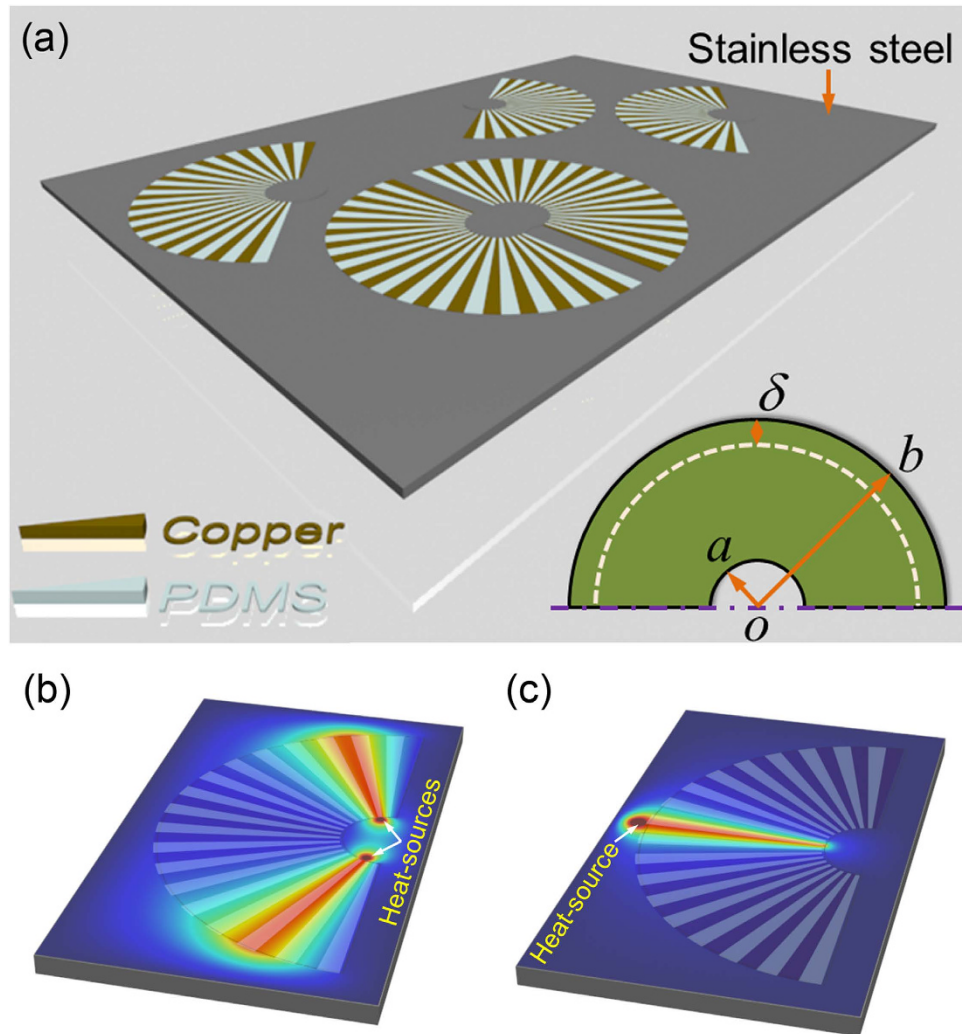
Figure 1. (**a**) Schematic of a random cluster of sensu-shaped thermal metamaterial units made of two regular bulk materials. The inset schematically shows the transformation principle of thermal metamaterial unit. (**b**) Two heat-sources placed near the inner boundary of a thermal metamaterial unit, analogous to the performance of an optical hyperlens. (**c**) A heat-source placed near the outer boundary of a thermal metamaterial unit, demonstrating harvesting property.

in advanced control of heat conduction can be experimentally demonstrated by positioning and combining identical unit.

In this paper, we introduce a new class of thermal metamaterials composed of two regular materials in a simplified planar geometry. The thermal metamaterial unit, designed with transformation optics[25,26], is capable of manipulating thermal energy and heat flux in a versatile variety of fashions by positioning and combining identical unit *sensu*-elements (which is a traditional folding hand-fan in Japan). We experimentally demonstrate that the combination of thermal metamaterial units exhibits novel properties such as the creation of a uniform heating region, heat flux focusing, and heat flux concentration. On one hand, these proposed metamaterials are fabricated using regular materials and can hence be easily accessed and followed. On the other hand, these novel properties are remarkably robust to the geometrical sizing of the proposed metamaterials without having to change the material compositions.

Results

Figure 1(a) shows the schematic of a random cluster of *sensu*-shaped thermal metamaterial (SSTM) units made of two regular bulk materials. The design of a SSTM unit is based on transformation optics[25,26], which is schematically illustrated in the inset of Fig. 1(a). The semi-annular region ($b - \delta < r' < b$) in virtual space is extruded to a larger region ($a \leq r \leq b$) in real space, where the virtual space and real space are denoted as (r', θ', z') and (r, θ, z), respectively. The transformation equations can be expressed as $r = \frac{b-a}{\delta}(r' - b) + b$, $\theta = \theta'$, and $z = z'$. Then the thermal conductivity in the region ($a \leq r \leq b$) is
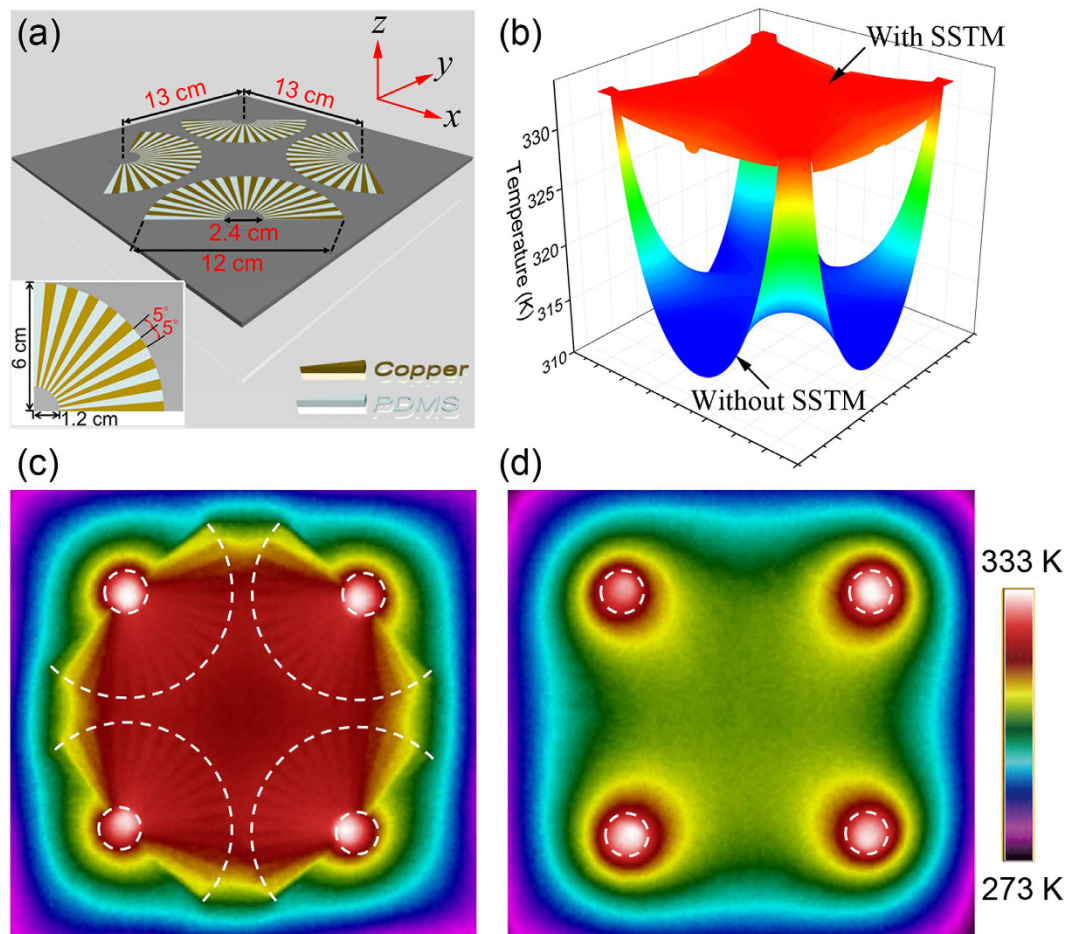
Figure 2. Experimental demonstration of forming a uniform heating region between four distant heat-sources enclosed by SSTM units. (**a**) Schematic of the fabricated sample. (**b**) Quantitative contrast of four distant heat-sources with and without SSTM. (**c**) Measured thermal profile of four distant heat-sources separately enclosed by SSTM units. (**d**) Measured thermal profile of four distant heat-sources without SSTM.

obtained as $\overleftrightarrow{\kappa} = \text{diag}\left(\frac{b-a}{\delta}\left(\frac{r'}{r}\right)^2 \quad \frac{\delta}{b-a}\right)$. When $\delta \to 0$, we obtain $\overleftrightarrow{\kappa} = \text{diag}(\infty \quad 0)$. It is rational to set $\kappa_r = \kappa_b 2^n$ and $\kappa_\theta = \kappa_b 2^{-n}$ so long as n is large enough, where κ_b is the thermal conductivity of the background. On the basis of effective medium theory (EMT), an anisotropic material may be practically realized by alternately stacking two materials A and B in the azimuthal direction. For practical realization, when the background is stainless steel, we choose copper and polydimethylsiloxane (PDMS) as materials A and B, respectively. Thus we can obtain the SSTM unit composed of 18 copper wedges and 18 PDMS wedges, shown in Fig. 1(a). The conductivities of copper, PDMS, and stainless steel are $\kappa_{Cu} = 394$ W/Km, $\kappa_{PDMS} = 0.15$ W/Km, and $\kappa_b = 16$ W/Km, respectively. We choose $a = 1.2$ cm and $b = 6$ cm for both simulations and experiments throughout.

To understand the functionalities of the SSTM unit, numerical simulations based on finite element modelling are demonstrated in Fig. 1(b,c). In the simulation setup, the four sides of the stainless steel (background) are set as fixed temperature at 0 °C. The top and bottom surfaces are set as adiabatic boundary. This ensures that the heat is mainly conducted rather than convected. When two point heat-sources are placed near the inner boundary of a SSTM unit, the simulated thermal profile is shown in Fig. 1(b). It is clearly seen that the thermal fields of the two heat-sources are almost perfectly transferred from inner-boundary to outer-boundary, analogous to the performance of an optical or acoustic hyperlens[27–30]. In contrast to the conceptual thermocrystal superlens for near-field imaging[13], our scheme may provide a more effective strategy for far-field thermal imaging. Inversely, when a point heat-source is placed near the outer boundary of the SSTM unit, the thermal energy is transferred into the center with almost no attenuation, as shown in Fig. 1 (c). This example only represents a small part of the potential of an SSTM unit, and more interesting functionalities that could be achieved through the combination of SSTM units will be demonstrated in the following.

We first experimentally demonstrate how to form a uniform heating region between four distant heat-sources by separating and enclosing them with four of our SSTM units. The fabricated structure
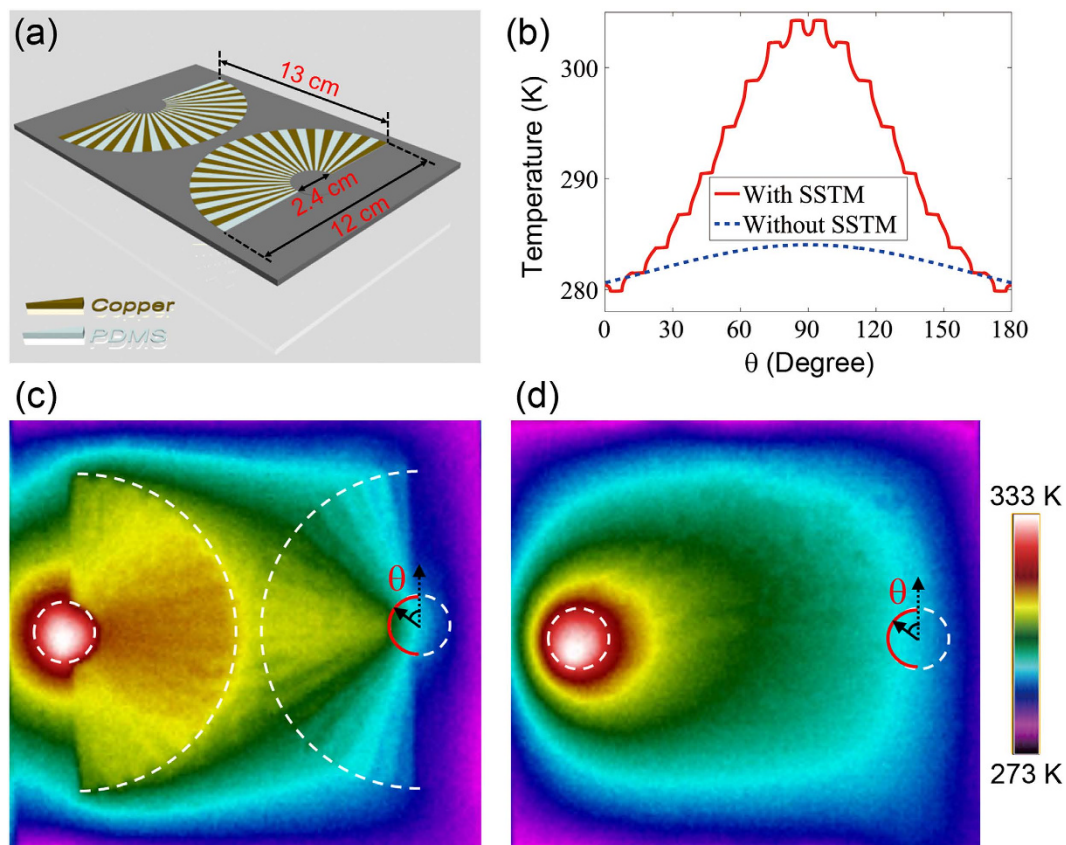
Figure 3. Experimental demonstration of thermal focusing. (**a**) Schematic of the fabricated sample. (**b**) Quantitative contrast of temperature distribution along semicircular red line in (**c**) and (**d**). (**c**) Measurement result of thermal focusing by enclosing a heat-source with SSTM unit and placing a second SSTM unit beside the first SSTM. (**d**) Measurement result of (**c**) without SSTM.

is schematically illustrated in Fig. 2(a). It is noted that we have thermally isolated all of the fabricated samples by using an approximately 100 μm thick layer of PDMS. The benefits of the PDMS layer are twofold -- heat convection by air is significantly reduced, and the PDMS layer on top of the sample is nearly "black" (i.e., 100% emissivity) for the wavelengths detected by the infra-red thermal imaging camera. The temperature distributions of four distant heat-sources with and without the SSTM units are quantitatively calculated in Fig. 2(b), in which the distance between two adjacent heat-sources (from the center of the left heat-source to the center of the right heat-source) is 13 cm. We can see that the valley-shaped temperature distribution for the case without the SSTM units become uniform after incorporating the four SSTM units. In the experimental setup, we use four brass cylinders with radius of 1 cm as heat-sources and the four boundaries are connected to a tank filled with ice water (0 °C). The four brass cylinders are connected to a hotplate fixed at 60°. The cross-sectional temperature profile is captured with a Flir i60 infrared camera. The measured results with and without SSTM units are shown in Fig. 2(c,d), respectively, which is as expected and agrees very well with the theoretical results in Fig. 2(b). From the coordinate transformation perspective, this is because the geometrical size of heat-sources have been enlarged by $b/a = 5$ times by using the SSTM. This property may find potential application in medical techniques like thermal therapy, where uniform heating is required over a body region.

A natural question is whether a uniform heating region can be formed by only using copper of the same size. To answer this question, we simulated the case in which the SSTM units are replaced by four copper quadrants of the same size as that of Fig.2(a); see Fig. S1 in Supplementary Materials. It is clearly demonstrated that *sensu*-patterned copper exhibits higher temperature and better heating uniformity performance than the unpatterned bare copper counterparts of the same size overall. It is also important to examine the performance of SSTM cluster in Fig. 2(a) with larger distance between two adjacent units, which is demonstrated in Fig. S2 in Supplementary Materials. For quantitative comparison, the temperature of the center is marked out. In general, the performance is naturally degraded with an increase in *d*. In all individual cases of different separation distances, the temperature distribution for the case with SSTM is always much higher than the case without SSTM.

We next experimentally demonstrate heat flux focusing by using SSTM units. Consider a heat-source (brass cylinder) being enclosed by a SSTM unit, and a second SSTM is placed beside the first SSTM
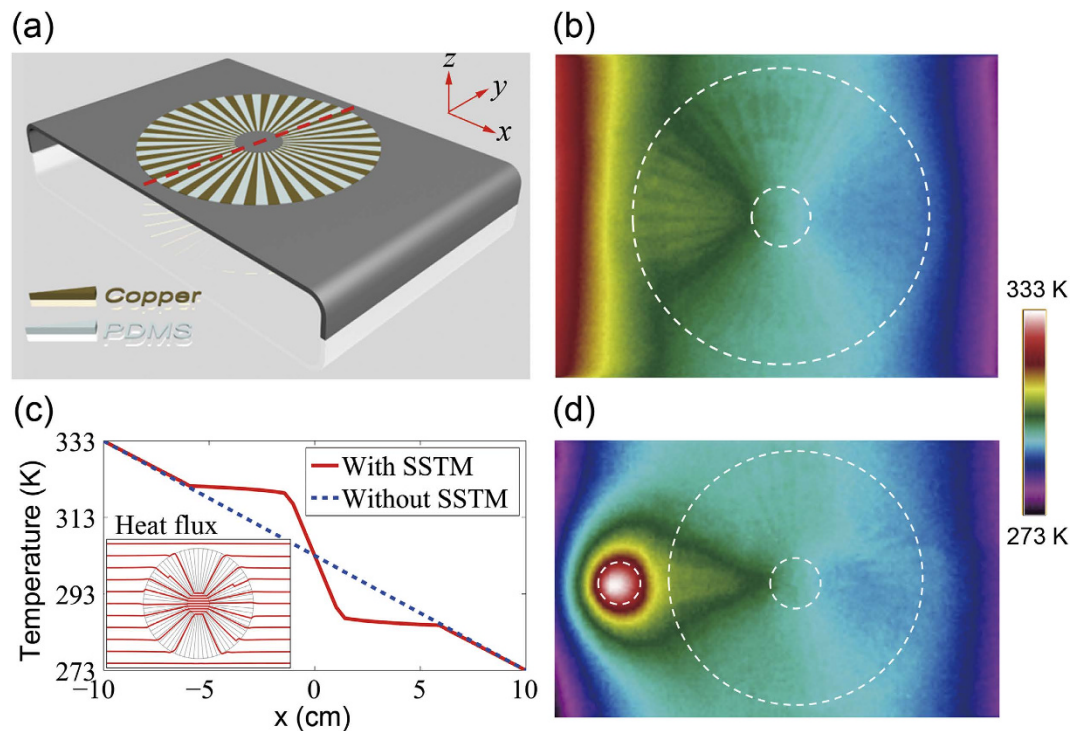
Figure 4. Experimental demonstration of an efficient thermal concentrator. (**a**) Schematic of the fabricated concentrator by the combination of two SSTM units. (**b**) Experimental verification of concentrating property in uniform thermal field. (**c**) Calculated temperature distribution along x-axis. The inset shows the heat flux lines. (**d**) Experimental verification of concentrating property in the presence of a point heat-source, emitting cylindrical heat fronts.

unit. We want to see that the enhanced thermal field of the heat-source is harvested by the second SSTM unit and focused into its center. The fabricated structure is schematically illustrated in Fig. 3(a). A brass cylinder with radius of 1 cm is placed at the center of the left SSTM unit and the four boundaries are connected to ice water (0 °C). The image captured by the infrared camera is shown in Fig. 3(c). For contrast, we measured the case where the two SSTM units are absent, as shown in Fig. 3(d). The temperature distribution along the semicircular red line in Fig. 3(c,d) is also calculated in Fig. 3(b), which agrees well with the experiment. Assuming the heat-source (placed in the first dotted circle) acts as a transmitter and the second dotted circle as a receiver, it is clear that the heat has been directed from the transmitter to the receiver by using the SSTM. When a thermal sensor is placed in the receiver position, the temperature is greatly enhanced, thus increasing the sensitivity of the temperature measurement. We also examine the cases where the SSTM units are replaced by copper wedges or copper quadrants (see Fig. S3 in Supplementary Materials). Obviously, there is no focusing effect with bare copper.

Moreover, we demonstrate an efficient heat flux concentrator by positioning two identical SSTM units. A concentrator is achieved by a combination of two back-to-back SSTM units, as shown in Fig. 4(a). For the measurement of the concentration effect, local heating on the left side is achieved by a hot plate fixed at 60 °C, and the right side is connected to a tank filled with ice water (0 °C). The experimental result on heat flux concentration is presented in Fig. 4(b), which clearly shows the significant role of the SSTM's presence. Nearly all heat flux in the region $(0 \leq r \leq b)$ is concentrated into the inner core $(0 \leq r \leq a)$ without any reflection and distortion, indicating nearly perfect concentration. For quantitative comparison, the temperature distributions along x-axis are presented in Fig. 4(c) for both cases (i.e., with and without SSTM), which clearly reveals that the presence of SSTM (solid line) confines and builds up the temperature within the central area more efficiently than the case without the SSTM (dashed line). We also examine the concentration behavior in the presence of a point heat-source, as shown in Fig. 4(d). In the experimental setup of Fig. 4(d), the left and right boundaries are connected to ice water (0 °C). Fig. 4(d) demonstrates the effectiveness of the proposed scheme in a non-uniform thermal field. In parallel, we study the cases in which the SSTM units are replaced by copper or PDMS, as shown in Fig. S4 in Supplementary Materials. Obviously, there is no concentration effect with bare copper or PDMS. Beyond the thermal regime, it is noted that *dc* electric field concentrator based on resistor networks[31] and *dc* magnetic field concentrator based on superconductor- ferromagnetic metamaterials[32,33] have been demonstrated recently.

Discussion

The SSTM concept can be extended -- we find that the proposed SSTM approach can also be applied to manipulate *dc* currents, which has been numerically verified in Fig. S5 in Supplementary Materials. In the simulation setup, we use the same geometrical parameters and material components as those in the thermal regime. This means that the proposed SSTM is able to manipulate both thermal fields and *dc* currents simultaneously, demonstrating bifunctional property[34,35].

In summary, we have proposed a new class of thermal metamaterials by using two regular bulk materials (copper and PDMS), and experimentally demonstrated its unique properties in terms of forming a uniform heating region, heat flux focusing, and concentration. These novel properties are robust to geometrical sizing of the SSTM unit whether scaled up or down. More interestingly the proposed SSTM is capable of manipulating both thermal field and *dc* currents simultaneously, exhibiting multi-functional property. Our scheme may find straightforward applications in technological devices such as thermoelectric devices, solar cells, thermal sensors, thermal imagers, as well as in thermal therapy applications. Our results can also provide novel ways to control other fields, e.g., dc magnetic fields, spin waves in spintronic devices, electrons in semiconductors.

Methods

The numerical simulations are performed by a commercial finite element method solver COMSOL Multiphysics. The SSTM unit, embedded in the stainless steel, is fabricated with 18 copper wedges and 18 PDMS wedges. The conductivities of copper, PDMS, and stainless steel are $\kappa_{Cu}=394$ W/Km, $\kappa_{PDMS}=0.15$ W/Km, and $\kappa_b=16$ W/Km, respectively. We choose $a=1.2$ cm and $b=6$ cm for both simulations and experiments throughout. For measurements, the cross-sectional temperature profile is captured with a Flir i60 infrared camera.

References

1. Venkatasubramanian, R., Siivola, E., Colpitts, T. & O'Quinn, B. Thin-film thermoelectric devices with high room-temperature figures of merit. *Nature* **413**, 597–602 (2001).
2. Steele, B. C. & Heinzel, A. Materials for fuel-cell technologies. *Nature* **414**, 345–352 (2001).
3. Padture, N. P., Gell, M. & Jordan, E. H. Thermal barrier coatings for gas-turbine engine applications. *Science* **296**, 280–284 (2002).
4. Wang, P. *et al.* A stable quasi-solid-state dye-sensitized solar cell with an amphiphilic ruthenium sensitizer and polymer gel electrolyte. *Nat. Mater.* **2**, 402–407 (2003).
5. Tian, B. *et al.* Coaxial silicon nanowires as solar cells and nanoelectronic power sources. *Nature* **449**, 885–889 (2007).
6. Chiritescu, C. *et al.* Ultralow thermal conductivity in disordered, layered WSe$_2$ crystals. *Science* **315**, 351–353 (2007).
7. Li, N. B., Ren, J., Wang, L., Huang, P. & Li, B. Colloqium: Phononics: Manipulating heat flow with electronic analogs and beyond. *Rev. Mod. Phys.* **84**, 1045 (2012).
8. Terraneo, M., Peyrard, M. & Casati, G. Controlling the energy flow in nonlinear lattices: A model for a thermal rectifier. *Phys. Rev. Lett.* **88**, 094302 (2002).
9. Li, B., Wang, L. & Casati, G. Thermal diode: Rectification of heat flux. *Phys. Rev. Lett.* **93**, 184301 (2004).
10. Chang, C. W., Okawa, D., Majumdar A. & Zettl, A. Solid-state thermal rectifier. *Science* **314**, 1121–1124 (2006).
11. Li, B., Wang, L. & Casati, G. Negative differential thermal resistance and thermal transistor. *Appl. Phys. Lett.* **88**, 143501 (2006).
12. Wong, H. S. P. *et al.* Phase change memory. *Proc. IEEE* **98**, 2201–2227 (2010).
13. Maldovan, M. Narrow low-frequency spectrum and heat management by thermocrystals. *Phys. Rev. Lett.* **110**, 025902 (2013).
14. Maldovan, M. & Thomas, E. L. Simultaneous localization of photons and phonons in two-dimensional periodic structures. *Appl. Phys. Lett.* **88**, 251907 (2006).
15. Guenneau, S., Amra, C. & Veynante, D. Transformation thermodynamics: cloaking and concentrating heat flux. *Opt. Express* **20**, 8207–8218 (2012).
16. Guenneau, S. & Puvirajesinghe, T. M. Fick's second law transformed: one path to cloaking in mass diffusion. *J. R. Soc. Interface* **10**, 20130106 (2013).
17. Narayana, S. & Sato, V. Heat flux manipulation with engineered thermal materials. *Phys. Rev. Lett.* **108**, 214303 (2012).
18. Dede, E. M., Nomura, T., Schmalenberg, P. & Lee, J. S. Heat flux cloaking, focusing, and reversal in ultra-thin composites considering conduction-convection effects. *Appl. Phys. Lett.* **103**, 063501 (2013).
19. Schittny, R., Kadic, M., Guenneau, S. & Wegener, M. Experiments on transformation thermodynamics: Molding the flow of heat. *Phys. Rev. Lett.* **110**, 195901 (2013).
20. Ma, Y., Lan, L., Jiang, W., Sun, F. & He, S. A transient thermal cloak experimentally realized through a rescaled diffusion equation with anisotropic thermal diffusivity. *NPG Asia Mater.* **5**, e73 (2013).
21. Narayana, S., Savo, S. & Sato, Y. Transient heat flux shielding using thermal metamaterials. *Appl. Phys. Lett.* **102**, 201904 (2013).
22. Han, T. *et al.* Experimental demonstration of a bilayer thermal cloak. *Phys. Rev. Lett.* **112**, 054302 (2014).
23. Xu, H., Shi, X., Gao, F., Sun, H. & Zhang, B. Ultrathin three-dimensional thermal cloak. *Phys. Rev. Lett.* **112**, 054301 (2014).
24. Alù, A. Viewpoint: Thermal cloaks get hot. *Physics* **7**, 12 (2014).
25. Pendry, J. B., Schurig, D. & Smith, D. R. Controlling electromagnetic fields. *Science* **312**, 1780–1782 (2006).
26. Leonhardt, U. Optical conformal mapping. *Science* **312**, 1777–1780 (2006).
27. Jacob, Z., Alekseyev, L. V. & Narimanov, E. Optical Hyperlens: Far-field imaging beyond the diffraction limit. *Opt. Express* **14**, 8247–8256 (2006).
28. Liu, Z., Lee, H., Xiong, Y., Sun, C. & Zhang, X. Far-field optical hyperlens magnifying sub-diffraction-limited objects. *Science* **315**, 1686 (2007).
29. Jiang, W. X. *et al.* Broadband all-dielectric magnifying lens for far-field high-resolution imaging. *Adv. Mater.* **25**, 6963–6968 (2013).
30. Li, J, Fok, L., Yin, X., Bartal, G. & Zhang, X. Experimental demonstration of an acoustic magnifying hyperlens. *Nat. Mater.* **8**, 931–934 (2009).
31. Jiang, W. X., Luo, C. Y., Ma, H. F., Mei, Z. L. & Cui, T. J. Enhancement of current density by dc electric concentrator. *Sci. Rep.* **2**, 956 (2012).
32. Navau, C., Prat-Camps, J. & Sanchez, A. Magnetic energy harvesting and concentration at a distance by transformation optics. *Phys. Rev. Lett.* **109**, 263903 (2012).

33. Prat-Camps, J., Navau, C. & Sanchez, A. Experimental realization of magnetic energy concentration and transmission at a distance by metamaterials. *arXiv*:1308.5878 2013.
34. Li, J. Y., Gao, Y. & Huang, J. P. A bifunctional cloak using transformation media. *J. Appl. Phys*. **108,** 074504 (2010).
35. Moccia, M., Castaldi, G., Savo, S., Sato, Y. & Galdi, V. Independent manipulation of heat and electrical current via bifunctional metamaterials. *Phys. Rev. X* **4,** 021025 (2014).

Acknowledgements

Author Contributions

T.H. and C.W.Q. contributed in theoretical analysis and numerical simulation. T.H., X.B. and D.L. performed the measurements. T.H. and D.G. prepared the manuscript. All authors contributed to the analysis and revision of the manuscript. C.W.Q. supervised the project.

Additional Information

Supplementary information accompanies this paper at http://www.nature.com/srep

Competing financial interests: The authors declare no competing financial interests.

How to cite this article: Han, T. *et al.* Manipulating Steady Heat Conduction by *Sensu*-shaped Thermal Metamaterials. *Sci. Rep.* **5**, 10242; doi: 10.1038/srep10242 (2015).